THEORETICAL AND EXPERIMENTAL INVESTIGATION OF STRONGLY LOCALIZED PLASMONS ON TRIANGULAR METAL WEDGES FOR SUB-WAVELENGTH WAVEGUIDING

D. F. P. Pile[a], T. Ogawa[a], D. K. Gramotnev[b],

T. Okamoto[a], M. Haraguchi[a], M. Fukui[a], S. Matsuo[c]

[a]*Department of Optical Science and Technology, Faculty of Engineering, The University of Tokushima, Minamijosanjima 2-1, Tokushima 770-8506, Japan*

[b]*Applied Optics Program, School of Physical and Chemical Sciences, Queensland University of Technology, GPO Box 2434, Brisbane, QLD 4001, Australia.*

[c]*Department of Ecosystem Engineering, Graduate School of Engineering, The University of Tokushima, Minamijosanjima 2-1, Tokushima 770-8506, Japan*

Abstract

We report numerical analysis and experimental observation of strongly localized plasmons guided by a triangular metal wedge. Dispersion and dissipation of such wedge plasmons are analyzed using the finite-difference time-domain algorithm. Experimental observation is conducted by the end-fire excitation and near-field detection of the predicted plasmons on a 40° silver nano-wedge. Good agreement with the theoretically predicted propagation distances is demonstrated. Differences between the theoretical and experimental field distribution are explained by insufficient resolution of the near-field optical probe.

The diffraction limit of light[1-3] is a major obstacle on the way of achieving high degree of miniaturization and integration of optical devices and circuits. The main approach to overcome this problem is related to use of surface plasmons in metallic nano-structures, such as rectangular metallic nano-strips,[4-6] nano-rods,[3,7] nano-chains,[1,2,8] metallic gaps,[9] trapezium-like nano-wedges,[10] etc. Parabolic metal wedges[11] could also be used for the design of sub-wavelength waveguides, though such a possibility has not been specifically analyzed. Recently, a new type of strongly localized plasmon – channel plasmon-polariton (CPP) – has been investigated theoretically in metallic grooves.[12-16] The major features of CPPs in V-grooves include a unique combination of strong localization and relatively low dissipation,[13,14] single-mode operation,[14] possibility of nearly 100% transmission through sharp bends,[15] and high tolerance to structural imperfections.[16]

Only very few experimental attempts to investigate different types of plasmonic waveguides with sub-wavelength localization have been undertaken so far.[2,6,10] In particular, it has been shown that nano-chain waveguides are characterized by a very strong dissipation and short propagation distances (less than ~ 200 nm).[1,2,8,17] Rectangular nano-strip waveguides have significantly lower dissipation,[5,6] but the experimentally achieved plasmon localization was only just below the diffraction limit.[6] No experimental investigation of gap plasmon waveguides, nano-rods, CPPs or parabolic wedge modes has been undertaken so far.

Therefore, the aim of this letter is in numerical analysis and experimental observation and investigation of new strongly localized plasmons guided by triangular metal wedges, and evaluation of these structures for the design of efficient sub-wavelength waveguides.

The numerical analysis is carried out by means of the 3-dimensional (3D) finite-difference time-domain (FDTD) algorithm that was previously developed and used for the investigation of CPPs,[13-16] and the compact-2-dimensional (compact-2D) FDTD approach.[18,19] The latter has been extended to plasmonic waveguides with negative permittivity[19] by using the local Drude model.[13-16,20] The compact-2D FDTD algorithm appears to be highly efficient, and provides more accurate field distribution and wave vectors of guided plasmons. However, it cannot be used for irregular guides with bends, non-uniformities, etc. Therefore, we will be using both of the FDTD formulations with the artificial absorbing boundary conditions of the first-order Mur type at the edges of the computational window.[21]

The analyzed structure with a silver wedge of the angle θ and a rectangular aperture is presented in Fig.1a. Plasmons in this structure are generated by means of the end-fire excitation using a bulk wave with the electric field parallel to the z-axis, incident onto the end of the wedge at an angle 45° (Fig. 1a). The aperture is used to suppress scattered bulk waves and surface plasmons on the sides of the wedge.

In the absence of the aperture, the steady-state instantaneous field distribution along the wedge in the (x,z) plane, calculated using the 3D FDTD algorithm, displays a snake-like pattern of beats localized near the tip of the wedge (Fig. 1b). The strongly localized periodic field along the tip suggests the existence of a new type of localized plasmonic eigenmode – wedge plasmon (WP). The snake-like pattern is produced by interference of the WP and the surface plasmons on the sides of the wedge. Indeed, it can be found that the z-component of the electric field E_z in a WP is approximately antisymmetric with respect to the (x,y) plane (this also results from the representation of WPs by guided antisymmetric plate plasmons[22]). On the other hand, the incident generating bulk wave with the electric field parallel to the z-axis (Fig. 1a) tends to generate surface plasmons on the sides of the wedge with the same direction of the normal component of the electric field (symmetric field distribution). The interference

between the symmetric and antisymmetric distributions of the z-components of the electric fields results in the antisymmetric beat pattern (Fig. 1b).

This is confirmed by the Fourier analysis of the field at the tip (similar to that in [13,14]). Two distinct maximums in the Fourier spectrum of the field are obtained in Fig. 1b at the wave numbers $q_1 \approx 1.20 \times 10^7$ m^{-1} (WP) and $q_0 \approx 1.025 \times 10^7$ m^{-1} (surface plasmon at the silver-vacuum interface). This also suggests that the considered wedge supports only one (fundamental) WP mode. Higher modes would have produced more maximums in the Fourier spectrum, and this indeed happens when $\theta \leq 30^o$.

Generation of surface plasmons and WP occurs at the point of the end-fire excitation. Beyond this point, surface plasmons experience significant diffractional divergence. Therefore, if we place a small aperture onto the wedge at some distance from the point of the end-fire excitation, so that it blocks the diverged surface plasmons and lets only WP through, this should significantly reduce the beats in Fig. 1b. This is confirmed by Fig. 1c. Significant presence of scattered bulk and surface waves can be seen between the end of the wedge and the aperture ($0 < x < 1.6$ μm, Fig. 1c), whereas behind the aperture only the strongly localized WP propagates along the tip of the wedge. The Fourier analysis of the field at the tip behind the aperture shows that the maximum due to surface plasmons practically disappears from the spectrum.

Fig. 1d shows the effect of dissipation on WP. It can be determined that the intensity of the WP drops e times within the propagation distance $L_{\text{theory}} \approx 2.25$ μm which is noticeably larger than the wavelength of the plasmon and thus is sufficient for a range of nano-optics applications.[1,6,10]

The analysis of the end-fire excitation can only be conducted using the 3D FDTD algorithm, and the compact-2D formulation is not applicable in this case. At the same time, the compact-2D FDTD provides more accurate results for the field distribution and dispersion of localized plasmons.[19] The dependencies of WP wave

number on θ for a silver wedge in vacuum, obtained in the compact-2D and 3D FDTD formulations, demonstrate significant differences at $\theta < 30^o$ (Fig. 2a). This is due to low computational efficiency of 3D FDTD at small θ, and compact-2D FDTD is preferable.

Note that WP modes can only exist if θ is less than a critical angle $\theta_c \approx 102^o$ (Fig. 2a). If $\theta = \theta_c$, then $q_1 = q_0 \approx 1.025 \times 10^7$ m^{-1}, and the WP has infinite penetration depth (zero localization) along the sides of the wedge. If $\theta > \theta_c$, WP does not exist as a structural eigenmode, since it leaks into surface plasmons. This is similar to the existence of the upper critical angle for CPP modes in metallic grooves.[13-16]

An example of the field distribution in the fundamental WP mode in a cross-section perpendicular to the tip of the 40° silver wedge is presented in Fig. 2b. It can be seen that this wedge can indeed support a plasmon with strong sub-wavelength localization within the region of ~ 50 nm (Fig. 2b).

The experimental observation and investigation of WPs were undertaken in the structure shown in Fig. 3a. An ~ 1.3 μm silver film was evaporated onto a glass substrate. Four wedges with the height ~ 1 μm were fabricated in this film using the focused-ion beam lithography (FIB). The inevitable finite radius of the wedge tips was ~ 25 nm. Direct end-fire excitation of WP modes by a laser beam focused onto the end of a wedge led to significant interference of the scattered field with the WP field registered by a near-field scanning optical microscope (NSOM). In addition, spatial drift of the laser beam tightly focused onto the wedge end resulted in substantial fluctuations of the registered intensity of WP. Therefore, the end-fire excitation was achieved through micro-holes fabricated in the silver film by means of FIB in front of the wedges (Fid. 3a). A laser beam illuminates the holes from underneath the film, and its tight focusing is not required, since the incident and WP fields are separated by the silver film.

The aperture of the NSOM probe tip was $\approx$ 100 nm diameter with ~ 100 nm aluminum coating. The tip-to-sample distance during measurements was maintained at $\approx$ 10 nm by the shear force feedback. The near-field intensities of the generated WPs on the four wedges (Fig. 3a) are shown in Fig. 3b. It can be seen that the intensity of the optical signal registered by NSOM decays along the positive x-direction in a similar fashion for all wedges (Fig. 3b). The solid curve in Fig. 3c represents the experimentally measured intensity of the NSOM signals along the wedge located at z = 0 in Fig. 3b. Its comparison with the theoretical dependence obtained from the 3D FDTD formulation (dashed curve in Fig. 3c) shows that the experimental propagation distance for WP (at the 1/e level of its intensity) $L_{exp} \approx$ 1.5 μm is smaller than the predicted theoretical value L_{theory} = 2.25 μm. This can be explained by roughness and non-uniformities of the wedge near the tip, which results in additional radiative experimental energy losses. Another reason for this discrepancy may be related to larger dissipation in the silver film compared to the bulk metal, and the effect of FIB lithography on the optical properties of silver near the tip. Taking this into account, the agreement between the theory and experiment (Fig. 3c) can be regarded as good. It is also interesting to note that no electromagnetic waves were detected next to the micro-aperture opposite to the wedge (i.e., in the region x < − 1.2 μm, Fig. 3c).

Fig. 3d shows the intensity of the optical signal registered by NSOM when scanning perpendicular to the wedge at the distance x = 3 μm from the point of excitation (solid curve). For comparison, the corresponding theoretical dependence is also presented (dashed curve). The substantial difference between these dependencies is explained by the low resolution of NSOM tip (with an aperture of ~ 100 nm). In addition, this aperture is surrounded by the 100 nm Al coating, which may result in substantial perturbation of the WP field and distortion of the experimental results. Therefore, only the experimental dependencies of the decaying field along the wedge can be regarded reliable. However, the fact that NSOM has shown lateral localization of the field near the tip of the wedge in the region of ~ 300 nm (Fig. 3d) constitutes

another proof that WP modes have been successfully detected. This is because such a field distribution is not possible due to bulk or surface waves, which would have experienced strong diffractional divergence.

In summary, this paper has reported the numerical analysis and the first experimental observation of a new type of strongly localized plasmons propagating along the tip of a triangular metal wedge. Plasmon parameters and field structure were determined by means of two different FDTD formulations. In particular, it has been shown that WP modes do not exist if the wedge angle is larger than a critical angle (which for a silver wedge in vacuum and $\lambda_{vac} = 0.6328$ μm is $\approx 102^{o}$). Strong sub-wavelength localization of WP modes has been demonstrated, and reasonable propagation distances have been predicted, which makes WP modes a good candidate for the design of sub-wavelength plasmonic waveguides.

The first direct excitation of a nano-waveguide by bulk waves was successfully conducted. Physical reasons for the observed discrepancies with the theoretical predictions are suggested. The predicted and experimentally observed propagation distances are sufficient for the design of nano-scale interconnectors between nano-optical devices. Further increase of the propagation distances could be achieved by means of gain-assisted propagation (which could be achieved by surrounding the metal with a gain medium, as was proposed for surface plasmons[23]).

References

[1]   J. R. Krenn, Nature Mater. **2**, 210 (2003).

[2]   S. A. Maier, P. G. Kik, H. A. Atwater, S. Meltzer, E. Harel, B. E. Koel, and A. A. G. Requicha, Nature Mater. **2**, 229 (2003).

[3]   J. Takahara, S. Yamagishi, H. Taki, A. Morimoto, and T. Kobayashi, Opt. Lett. **22**, 475 (1997).

[4]   P. Berini, Phys. Rev. B **63**, 125417 (2001).

[5]   B. Lamprecht, J. R. Krenn, G. Schider, H. Ditlbacher, M. Salerno, N. Felidj, A. Leitner, and F. R. Aussnegg, Appl. Phys. Lett. **79**, 51 (2001).

[6]   J. R. Krenn, B. Lamprecht, H. Ditlbacher, G. Schider, M. Salerno, A. Leitner, and F. R. Aussenegg, Europhys. Lett. **60**, 663 (2002).

[7]   C. A. Pfeiffer, E. N. Economou, and K. L. Ngai, Phys. Rev. B **10**, 3038 (1974).

[8]   J. R. Krenn, A. Dereux, J. C. Weeber, E. Bourillot, Y. Lacroute, J. P. Goudonnet, G. Schider, W. Gotschy, A. Leitner, F. R. Aussenegg, and C. Girard, Phys. Rev. Lett. **82**, 2590 (1999).

[9]   K. Tananka and M. Tanaka, Appl. Phys. Lett. **82**, 1158 (2003); K. Tananka, M. Tanaka, and T. Sugiyama, Optics Express **13**, 256 (2005); B. Wang and G. P. Wang, Appl. Phys. Lett. **85**, 3599 (2004); B. Wang and G. P. Wang, Opt. Lett. **29**, 1992 (2004).

[10]   T. Yatsui, M. Kourogi, and M. Ohtsu, Appl. Phys. Lett. **79**, 4583 (2001).

[11]   A. D. Boardman, G. C. Aers, and R. Teshima, Phys. Rev. B **24**, 5703 (1981).

[12]   I. V. Novikov and A. A. Maradudin, Phys. Rev. B **66**, 035403 (2002).

[13]   D. F. P. Pile and D. K. Gramotnev, Opt. Lett. **29**, 1069 (2004).

[14]   D. K. Gramotnev and D. F. P. Pile, Appl. Phys. Lett. **85**, 6323 (2004).

[15]   D. F. P. Pile and D. K. Gramotnev, Opt. Lett. **30**, 1186 (2005).

[16] D. F. P. Pile and D. K. Gramotnev, Appl. Phys. Lett. **86**, 161101 (2005).

[17] S. A. Maier, M. L. Brongersma, and H. A. Atwater, Appl. Phys. Lett. **78**, 16 (2001).

[18] A. Asi and L. Shafai, Electron. Lett. **28**, 1451 (1992); A. Cangellaris, IEEE Microwave and Guided Wave Lett. **3**, 3 (1993); M. Qui, Microwave and Opt. Tech. Lett. **30**, 327 (2001).

[19] D. F. P. Pile, Appl. Phys. B (accepted).

[20] D. Fowers, Masters Thesis (University of Utah, Salt Lake City, Utah, 1994) (1994); D. Christensen and D. Fowers, Biosens. Bioelectron **11**, 667 (1996).

[21] G. Mur, IEEE Trans. Electromagn. Compat. **40**, 100 (1998).

[22] D. K. Gramotnev and K. C. Vernon, Phys. Rev. B (unpublished).

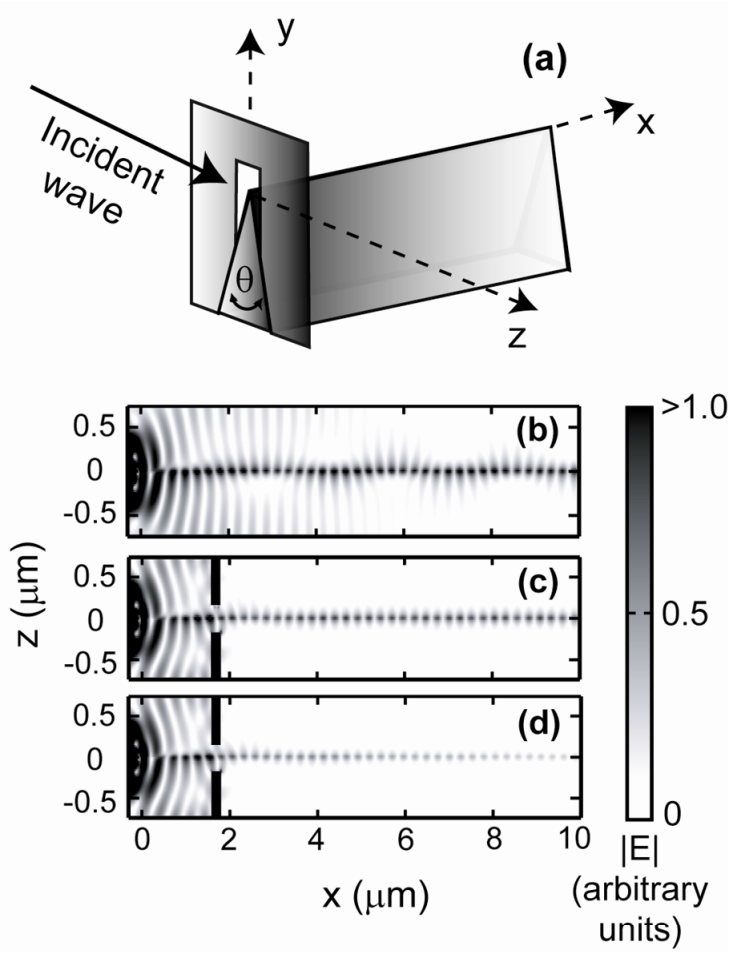[23] M. P. Nazhad, K. Tetz, and Y. Fainman, Optics Express **12**, 4072 (2004).

Fig.1. (a) A triangular silver wedge with the end-fire excitation of WP modes through an aperture for suppression of surface and bulk waves. The aperture in a ~ 200 nm thick silver film is ≈ 300 nm wide (along the z-axis) and its top edge is ≈ 170 nm above the tip of the wedge; the aperture is placed on the wedge at the distance ≈ 1.6 μm from its end (i.e., from the point of the end-fire excitation). (b-d) Distributions of the magnitude of the electric field in the (x,z) plane, calculated using the 3D FDTD method for the silver wedge with the angle θ = 40° in vacuum at the vacuum wavelength λ_{vac} = 0.6328 μm (He-Ne laser). (b) No aperture and no dissipation in the metal; the metal permittivity: ε_m = − 16.22. (c) In the presence of the aperture and in the absence of dissipation. (d) In the presence of both the aperture and dissipation: ε_m = -16.22 + 0.52i. The presented metal permittivities were determined using the local Drude model[20] with the electron charge density ρ ≈ − 7.684×10^9 C/m^3 and damping frequency f_d = 0 Hz (for (b,c)), and f_d ≈ 1.4332×10^{13} Hz (for (d)).
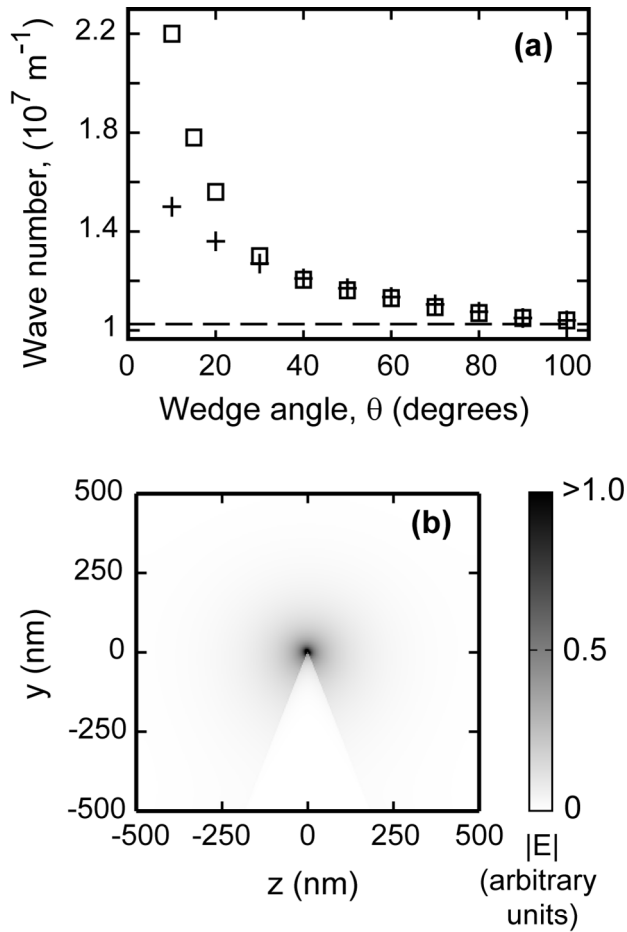
Fig. 2. (a) The dependencies of the wave number of the fundamental WP mode on wedge angle θ, calculated by 3D FDTD (crosses) and compact-2D FDTD (squares). The horizontal dashed line represents the wave number $q_0 = 1.025 \times 10^7 \ m^{-1}$ of the surface plasmons on the sides of the wedge. (b) The distribution of the magnitude of the electric field (compact-2D FDTD) in a cross-section perpendicular to the tip of the wedge. The structural and wave parameters are the same as for Fig. 1.
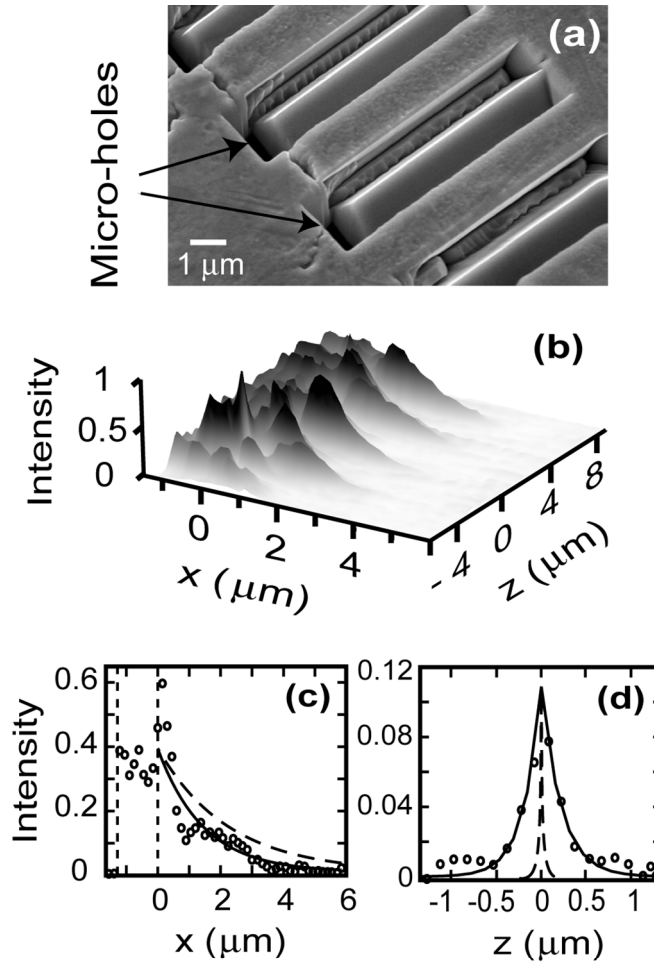
Fig. 3. (a) SEM image of the experimental structure with four wedges of ≈ 7 μm length in the silver film. (b) NSOM intensity of the optical signal along the four wedges (the x-axis is parallel to the wedges). The structure is excited by a beam ($\lambda_{vac} = 0.6328$ μm) of circular polarization incident onto the micro-holes (-1.2 μm $< x < 0$ μm) from underneath the silver film (Fig. 3a) at an angle of 45° to the x-axis. The point of the end-fire excitation: $x = 0$. (c) NSOM intensity of the optical signal along the tip of the 40° wedge (at $z = 0$ in Fig. 3b) with the exponential fit to the experimental points (solid curve) in the waveguide region. The region of the micro-aperture is shown by the two vertical dotted lines. Dashed curve: theoretical dependence from 3D FDTD. (d) NSOM detected intensity of the optical signal versus z-coordinate taken at $x \approx 3$ μm with the distance from the sample surface to the NSOM tip maintained at ≈ 10 nm. Solid curve: exponential fit to the experimental points. Dashed curve: theoretical distribution from the compact-2D FDTD.